Poropat, L., Dobslaw, H., Zhang, L., Macrander, A., Boebel, O., Thomas, M. (2018): Time Variations in Ocean Bottom Pressure from a Few Hours to Many Years: in situ Data, Numerical Models, and GRACE Satellite Gravimetry. - *Journal of Geophysical Research*, *123*, 8, pp. 5612—5623.

DOI: http://doi.org/10.1029/2018JC014108

Journal of Geophysical Research: Oceans

RESEARCH ARTICLE
10.1029/2018JC014108

Key Points:
- In situ measurements of ocean bottom pressure from various sources are assembled into one database
- Variability at periods from 3 to 30 days is very well explained by a global numerical model experiment
- GRACE gravity fields are closer to in situ bottom pressure after appropriate postprocessing

Correspondence to:
L. Poropat,
poropat@gfz-potsdam.de

Citation:
Poropat, L., Dobslaw, H., Zhang, L., Macrander, A., Boebel, O., & Thomas, M. (2018). Time variations in ocean bottom pressure from a few hours to many years: In situ data, numerical models, and GRACE satellite gravimetry. *Journal of Geophysical Research: Oceans*, *123*, 5612–5623. https://doi.org/10.1029/2018JC014108

Received 24 APR 2018
Accepted 29 JUN 2018
Accepted article online 12 JUL 2018
Published online 15 AUG 2018

Time Variations in Ocean Bottom Pressure from a Few Hours to Many Years: In Situ Data, Numerical Models, and GRACE Satellite Gravimetry

L. Poropat[1], H. Dobslaw[1], L. Zhang[1], A. Macrander[2], O. Boebel[3], and M. Thomas[1,4]

[1]Department 1: Geodesy, GFZ German Research Centre for Geosciences, Potsdam, Germany, [2]Marine and Freshwater Research Institute, Reykjavík, Iceland, [3]Alfred Wegener Institute for Polar und Marine Research, Bremerhaven, Germany, [4]Institute of Meteorology, Freie Universität Berlin, Berlin, Germany

Abstract In situ ocean bottom pressure (OBP) obtained from 154 different locations irregularly scattered over the globe is carefully processed to isolate signals related to the ocean general circulation and large-scale sea level changes. Comparison against a global numerical ocean model experiment indicates poor correspondence for periods below 24 hr, possibly related to residual tidal signals and small timing errors in the atmospheric forcing applied to the ocean model. Correspondence increases rapidly for periods between 3 and 10 days, where wind-driven dynamics are already well understood and consequently well implemented into numerical models. Coherence decreases again for periods around 30 days and longer, where processes not implemented into ocean general circulation models as barystatic sea level changes become more important. Correspondence between in situ data and satellite-based OBP as obtained from the Gravity Recovery and Climate Experiment (GRACE) German Research Centre for Geosciences RL05a gravity fields critically depends on the postprocessing of Level-2 Stokes coefficients that also includes the selection of appropriate averaging regions for the GRACE-based mass anomalies. The assessment of other available GRACE Level-2 products indicates even better fit of more recent solutions as ITSG-Grace2016 and the Center for Space Research and Jet Propulsion Laboratory RL05 mascons. In view of the strong high-frequency component of OBP, however, a higher temporal resolution of the oceanic GRACE products would be rather advantageous.

1. Introduction

Temporal variations in the ocean bottom pressure (OBP) field and its spatial gradients reflect a wide range of dynamic regimes in the ocean. Barotropic ocean tides on frequencies from subdaily (Ray, 2013) to long-period (Ray & Erofeeva, 2014) dominate the field but can be readily separated due to the monocromatic character of the dominant partial tides. Other barotropic waves as, for example, tsunamis excited by offshore earthquakes or submarine landslides, have a rather transient OBP signature (Milburn et al., 1996). Low-frequency changes in globally averaged OBP reflect the global mean barystatic sea level rise due to water influx from continental storages (Chambers, 2006). The majority of variability at time scales from days to many years, however, is related to the thermohaline and wind-driven circulation in the world's ocean, which is represented numerically in global and regional ocean general circulation models (Bingham & Hughes, 2008a).

OBP is routinely measured for diverse purposes, both by means of research campaigns or as part of long-term operational networks. The Deep-ocean Assessment and Reporting of Tsunamis (DART) network monitors OBP throughout the Pacific to facilitate tsunami early warning (Meinig et al., 2005). Transport variability of the Antarctic Circumpolar Current (ACC)—the largest ocean current system on the globe—has been monitored in Drake Passage already 40 years ago (Nowlin et al., 1977) and continues until present days also with the help of in situ OBP recorders (Meredith et al., 2011). The dynamics of the Kuroshio extension off the Japanese coast—a region characterized by high eddy kinetic energy due to the confluence of warm, salty subtropical and cold, fresh subpolar waters—were recently studied in detail with an array of current meters and pressure recording inverted echo sounders (Bishop & Watts, 2014). And finally, the Atlantic Meridional Overturning Circulation—responsible for poleward heat transport and the associated rather mild climate in western Europe—is monitored routinely by the RAPID array at 26°N with a series of in situ OBP sensors aligned along the gradient of the continental shelf (McCarthy et al., 2015).

Observations of ocean bottom pressure are technically challenging since in situ sensors are required to detect variations of less than 1 hPa at depths of up to 10 km, which translates into a measurement sensitivity of 10^{-9} while being exposed to a highly corrosive environment. Sensors suitable for practical oceanographic purposes became only available at affordable prices about three decades ago (Watts & Kontoyiannis, 1990), which subsequently allowed the deployment of a very irregularly distributed global network of OBP recorders. More recently, activities are underway to make OBP observations a part of newly laid out transcontinental communication cables, which would provide continuous in situ measurements with more homogeneous spatial distribution, including areas far away from the coasts, which currently have very few OBP measurements (Howe & Workshop Participants, 2015).

Besides distributing in situ sensors throughout the global oceans, OBP can be also observed remotely from satellites. The gravity mission GRACE (Gravity Recovery and Climate Experiment) launched in March 2002 consists of two identical satellites trailing each other in a near-circular orbit at initially 500 km altitude. The satellites are separated by approximately 220 km and measure their relative positions by means of a highly accurate intersatellite, K band microwave ranging system (Tapley et al., 2004). The GRACE mission has ended its science operation phase in the year 2017, but the follow-on mission GRACE-FO (Flechtner et al., 2016) was successfully launched on 22 May 2018.

In this paper, we are going to contrast OBP from in situ sensors against output from a numerical ocean circulation model and the results of the GRACE mission in order to evaluate the current level of consistency between remotely sensed and in situ OBP as well as numerical models. The paper is structured as follows: In section 2, we describe the in situ OBP data and the processing we apply to it, whereas in situ and simulated OBP data are compared in section 3. Subsequently, we describe the comparison of the in situ and satellite-based OBP and discuss necessary adjustments applied to the GRACE data before it can be contrasted with in situ observations (section 4), assess the differences between various spherical harmonics and mascon GRACE solutions (section 5), followed by some conclusions given in section 6.

2. OBP From In Situ Observations

Ocean bottom pressure is the combined pressure caused by the weight of the column of sea water and the atmosphere above it. We make use of data from globally distributed ocean bottom pressure recorders from various institutions initially compiled by Macrander et al. (2010). The data are taken from 167 different geographic positions irregularly scattered over all ocean basins with some bias toward the Northern Pacific Ocean. Time series from every station are visually inspected for drifts and discontinuities. Long-term drifts are present in some OBP in situ time series due to the mechanical creep of materials subjected to high stress (Watts & Kontoyiannis, 1990). Since a few stations had a significant nonlinear drift at the beginning or the end of its time series, short segments of data were discarded. Long-term trends, as well as the remaining drifts, are removed with a quadratic fit. Discontinuities are sometimes present in the time series due to recovery and redeployment of sensors for data recovery, battery replacement, and general maintenance. After the drifts and trends are removed from every segment of data separately, a Heaviside function is fitted and removed to every discontinuity.

Data are subsequently cleared from outliers by applying a 5-sigma criterion. Temporal sampling is reduced to 1 hr for all stations that provide subhourly sampled data. Tidal signals are removed from the time series with the T_TIDE package for classical harmonic analysis (Pawlowicz et al., 2002). The number of tidal constituents is automatically chosen and ranges from 17 for the shortest time series to 68 for time series with the length of $\sim$1 year. The longest tidal period fitted to every in situ time series is the fortnightly constituent MSF with a period of 354.37 hr. The annual tide SA with period of 365.26 days is removed only from the longest time series. Because T_TIDE is best suited for time series with 1 year length since the implemented nodal corrections may not be accurate enough for longer time series, all time series significantly longer than 1 year were separated into smaller segments prior to de-tiding. Finally, data series from the same geographical position but different deployments of the same sensor or even different sensors operated in succession are stacked into one time series by reducing each segment to zero mean. For this study, data from the time period 2002–2010 at 154 different stations with a varying length of the individual time series are considered (Figure 1).

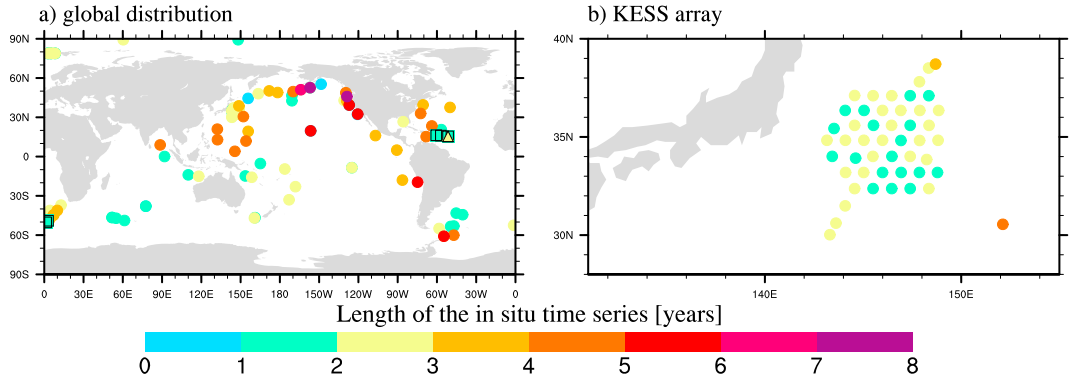

Figure 1. Time series length and temporal sampling for all ocean bottom pressure in situ stations utilized in this study in the world oceans (a) and in the Kuroshio region off the coast of Japan (b). Circles represent locations with in situ measurements with hourly or higher temporal sampling, triangles 12-hourly and squares 24-hourly sampling. KESS = Kuroshio Extension System Study.

3. OBP From an OGCM Experiment

In the following, we utilize results from a recent numerical ocean circulation model experiment to assess the plausibility of the observed OBP. We apply the ocean component of the coupled Earth System Model from the Max Planck Institute for Meteorology in Hamburg (Jungclaus et al., 2013) in a configuration with moderate horizontal resolution (tripolar grid with approximately 1° grid spacing) and 40 layers in the vertical. The model is initialized from climatological temperature and salinity distributions (Boyer et al., 2005), forced with 3-hourly atmospheric data from ERA-Interim starting in 1979 and operational analysis data of ECMWF from 2007 onward. The particular experiment is described in more detail by Dobslaw et al. (2017). Since it is not constrained by observations, the model experiment is fully independent of the in situ OBP data introduced above.

Model output is disaggregated into five different frequency bands by means of a series of fourth-order Butterworth filters with cutoff periods of 1, 3, 10, and 30 days, and the variability for each of the frequency bands is plotted in terms of root-mean-square (rms) values calculated over the period 2003–2012 (Figure 2). Subdaily periods are dominated by basin-wide barotropic gravity waves that cause the largest bottom pressure variability in shallow shelf areas and semienclosed seas. Variability generally increases in the 1- to 3-day period band, where transient weather patterns start to modulate the ACC and consequently induce bottom pressure variability almost everywhere in the Southern Ocean. For 3–10 days, we note distinct regions in the ACC area showing an enhanced OBP variability, which is related to the particular resonance characteristics of the regional bathymetry at those frequencies. Those resonances are changing when moving to even longer periods, but the particular sensitivity of individual locations in the Southern Oceans to certain periodicities in the atmospheric forcing remains the dominant driver of OBP variability.

We finally note that the variability obtained from low-pass filtering the modeled OBP time series with a fourth-order Butterworth filter somewhat differs from the results obtained from monthly-mean averages. Calculating unweighted monthly-mean values from a time series effectively corresponds to convolving a time series with a rectangular weighting function, whose Fourier transform exhibits substantial side lobes at periods shorter than 30 days. This is reflected in the plots, showing, for example, diminished variability in the Bellingshausen Basin northward of the Amundsen Sea in the monthly-mean estimates compared to the 30-days low-pass filtered series. Similar deviations are also visible for other regions of the world.

Model output at 3-hourly temporal sampling is subsequently contrasted against the observed in situ OBP. Note that 12 frequencies associated with atmospheric and oceanic pressure loading tides at periods from 8 to 24 hr have been estimated and removed from the modeled data set in order to retain the nontidal variability only. Model data is extracted at each OBP in situ station by means of bilinear interpolation from the four nearest grid points. We calculate relative variance changes $r(m)$ of the observations o when the modeled quantity m is subtracted:

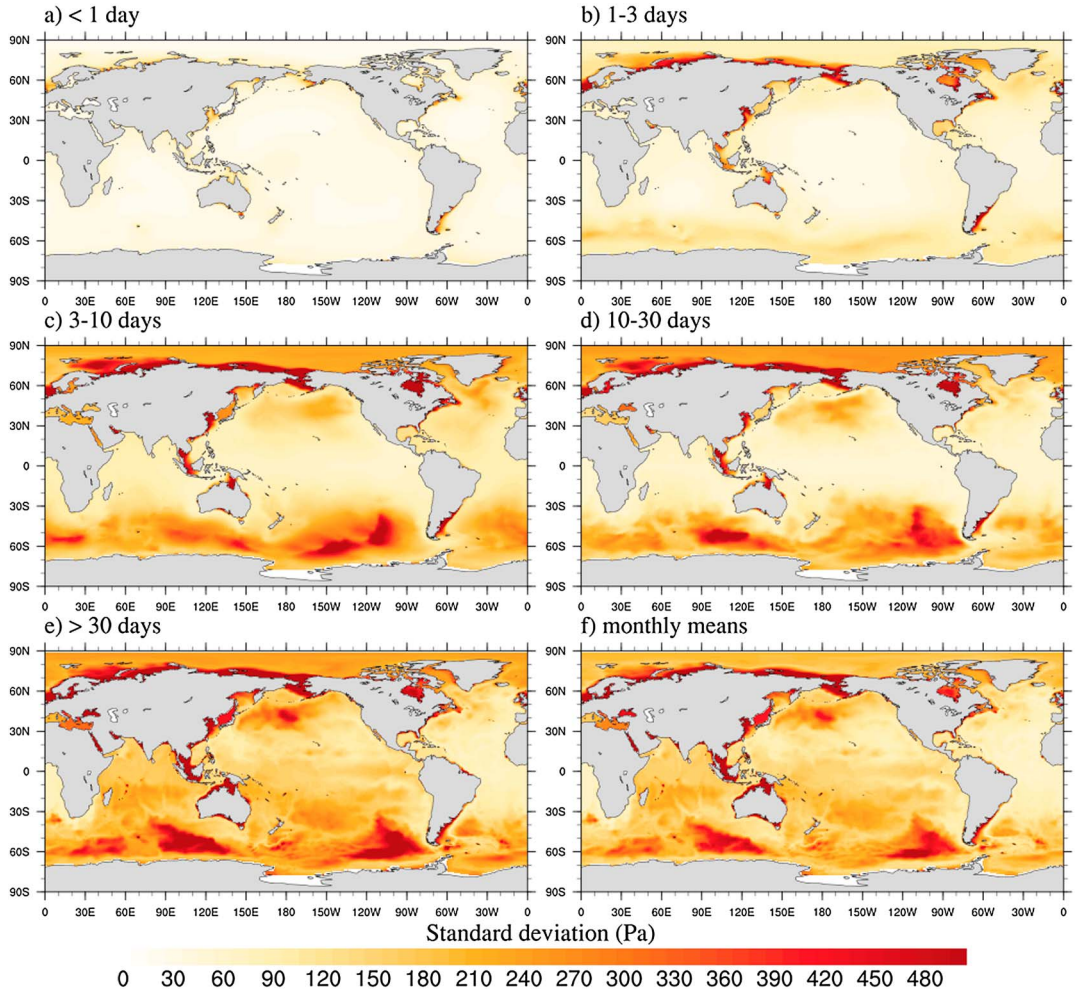

Figure 2. Root-mean-quare (rms) values of 3-hourly ocean bottom pressure variability simulated with MPIOM over the time period 2003–2012 separated into five different frequency bands by means of fourth-order Butterworth filters: (a) periods shorter than 24 hr; (b) 1–3 days; (c) 3–10 days; (d) 10–30 days; and (e) longer than 30 days. Additionally, the rms calculated from monthly-mean ocean bottom pressure averages from the same model experiment is provided (f).

$$r(m) = \frac{D^2(o) - D^2(o-m)}{D^2(o)}, \tag{1}$$

where $D^2(o)$ indicates the variance of the in situ observations o, and $D^2(o-m)$ the residual variance after subtracting the model. Since moving-window filters distort data toward both ends of a time series, and since in situ records typically contain many data gaps of varying duration, small gaps are linearly interpolated before filtering. Note that those interpolated epochs are again removed before calculating explained variances. Data gaps present in the in situ time series are considered in the simulated data as well prior to the calculation of relative explained variances to ensure that both the in situ and simulated time series have exactly the same number of data points.

For the most rapid variations at periods shorter than 24 hr (Figure 3a), we note almost no agreement between model and observations. Observed variability is likely affected by residual tidal signals not properly removed. Small timing errors in the onset of weather systems and associated fronts present in the atmospheric data consequently also cause a delayed OBP response in the numerical ocean model. Note further that forcing data are only provided to the ocean model every 3 hr with linear interpolation in time to the actual time step of the model of 90 min, which further reduces the quality of simulated OBP at subdiurnal periods. Correspondence increases, however, for periods between 1 and 3 days (Figure 3b) with most of the stations having small positive relative explained variance. Most prominent examples are the Arctic Ocean (60% of the variability

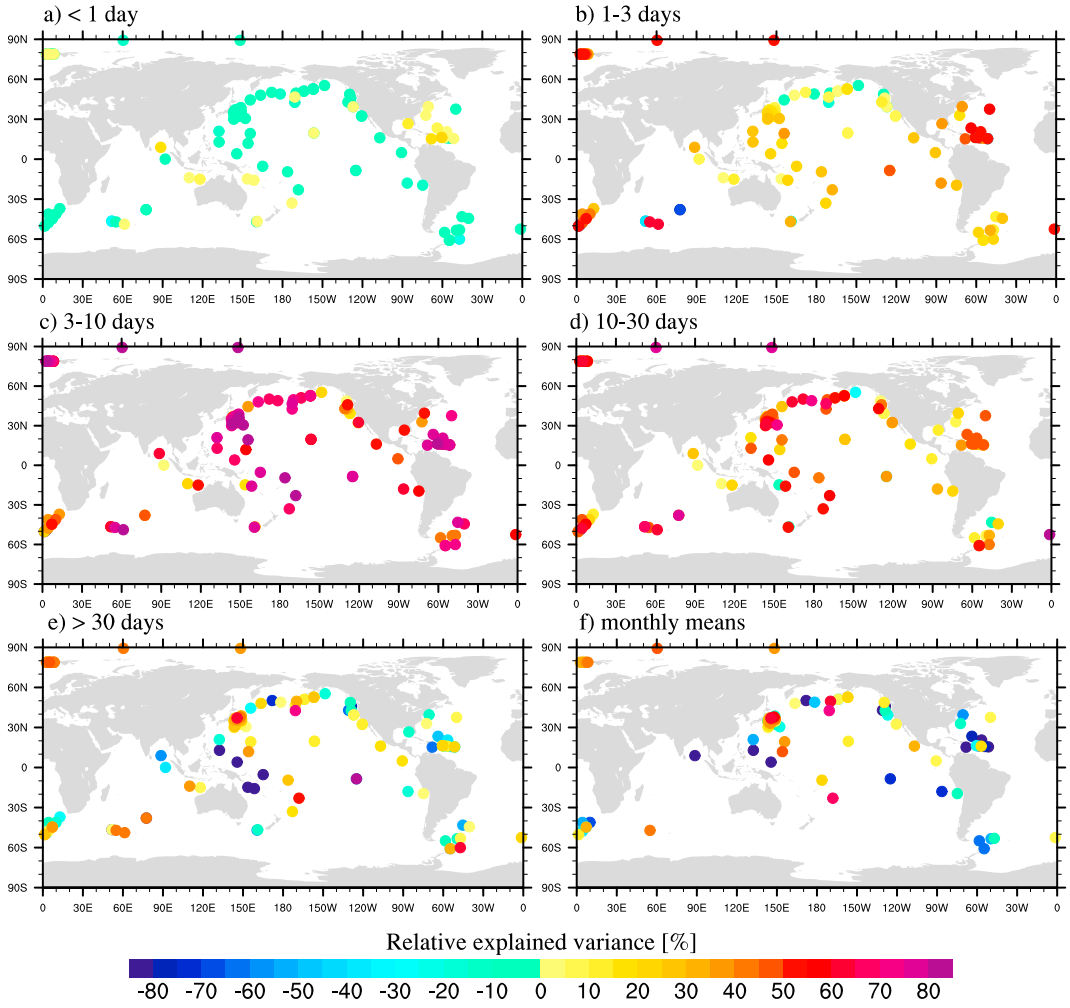

Figure 3. Percentage of variance in OBP observed at in situ stations that is explained by a numerical ocean model experiment with MPIOM for periods (a) shorter than 24 hours; (b) between 1 and 3 days; (c) between 3 and 10 days; (d) between 10 and 30 days; and (e) longer than 30 days as separated by means of 4th order Butterworth filters. In addition, the relative explained variance for monthly-mean estimates is given (f).

observed in that frequency band is explained by the model), the tropical Atlantic (50%), and the ACC region, in particular, in the sector south of Africa (up to 50%).

For periods between 3 and 10 days (Figure 3c), we note exceptionally good correspondence between in situ observations and the numerical model. Relative explained variances frequently exceed 70% even at locations close to the coast and in areas with steep gradients in bathymetry. All considered stations have positive explained variance, indicating skill of the ocean model at every single location where in situ OBP observations are available. OBP variability in this frequency band is largely dominated by the wind-driven circulation, thereby suggesting that the physics behind that process at, in particular, large spatial scales, are already well understood and subsequently well implemented into MPIOM.

When moving toward longer periods of up to 30 days (Figure 3d), however, explained variances are somewhat lower again. At those frequencies, density-related effects have an increasingly growing influence on the in situ observations. Nevertheless, all but three stations still have positive explained variances. For OBP variations at periods of 30 days and longer (Figure 3e), however, the correspondence between the numerical model and the observations is rather poor. This might be related to the subtraction of long-term quadratic signals and the reduction of data gaps in the observations as described above; to the fact that seasonal and interannual sea level variations associated with self-attraction and loading (Tamisiea et al., 2010) and the influx of water from the continents (Bergmann-Wolf et al., 2014) are not considered in the model; and to OBP signals associated

with time variations in the meridional overturning circulation that are certainly not captured by the model to its full extent (Bingham & Hughes, 2008b).

We finally note that utilizing monthly-mean values (Figure 3f) instead of 3-hourly data that is low-pass filtered with a 30-day cutoff period alters the results in a nonnegligible way. As indicated above, boxcar moving average filters retain variability at higher frequencies and give values toward both ends of the averaging window higher weights than theoretically desirable. Due to the additional influence of data gaps in the in situ series, the results change rather strongly for some of the stations. This is particularly true in the vicinity of the ACC whose variability is dominated by the weather time scale. Here we note a substantial degradation of the fit between model and in situ observations when monthly means are considered instead of low-pass filtered time series. Furthermore, some stations need to be discarded because they do not contain sufficiently long time series when monthly-mean values are considered.

4. OBP From GRACE Satellite Data Processed at GFZ

The GRACE satellite mission consists of two identical satellites equipped with a suite of instruments required to map the Earth's gravity field from space. Those precise sensors include a microwave tracking system to measure range and range rates between the two satellites; an upward looking GPS receiver to determine the spacecraft's position relative to a constellation of navigation satellites; an accelerometer with three sensitive axes mounted at the center of mass of each satellite to distinguish between gravitational and nongravitational forces; and two star cameras to quantify the orientation of the satellite with respect to inertial space. Data accumulated over 30 days are typically processed into a global gravity field with a spatial resolution of about 500 km. Over the whole lifetime of the GRACE mission, individual gravity field solutions for more than 160 different months have been calculated and made publicly available as so-called Level-2 science products in terms of Stokes coefficients. The most recent data product officially released by German Research Centre for Geosciences (GFZ) is RL05a (Dahle et al., 2016).

Differences from month to month in the gravity field are related to changes in the mass distribution on Earth and can thus be converted into surface mass anomalies or consequently OBP variations. Starting from Level-2 Stokes coefficients, degree-1 terms and C_{20} have to be added from auxiliary sources; subsurface geophysical signals associated with glacial isostatic adjustment or coseismic deformations need to be removed; and spatially anisotropic and temporally varying filtering is required to reduce the effects of correlated noise contained in the solutions at, in particular, smaller spatial scales. Finally, gravity changes are inverted into OBP anomalies by assuming an infinitely thin layer of time variable mass at the surface of the reference ellipsoid, and the monthly mean of the nontidal atmosphere-ocean mass variability removed during the dealiasing process is added back.

Such global OBP grids with a typical spatial sampling of 1° are publicly available from NASA's TELLUS portal accessible at http://grace.jpl.nasa.gov. For the TELLUS data, C_{20} coefficients are replaced with a solution from Satellite Laser Ranging (Cheng et al., 2011); degree-1 coefficients are estimated using the method from Swenson et al. (2008); a glacial isostatic adjustment correction has been applied based on the model from A et al. (2013); a destriping and a 500-km-wide Gaussian filter have been applied to the data (Swenson & Wahr, 2006); and land leakage is minimized by using an iterative procedure (Chambers, 2012). As an alternative access point to the public, GFZ has recently launched the GRAVIS portal available at http://gravis.gfz-potsdam.de, which is also providing Level-3 GRACE-based OBP grids based on the same series of GFZ RL05a Stokes coefficients. For the GRAVIS data, degree-1 coefficients are approximated according to Bergmann-Wolf et al. (2014); C_{20} is replaced with values from satellite laser ranging provided by Cheng and Ries (2013); GIA effects are subtracted by means of Paulson et al. (2007); coseismic and postseismic deformations of the largest earthquakes are estimated and subtracted (Tanaka et al., 2018); and the nonisotropic DDK-1 filter (Kusche et al., 2009) is applied to reduce the impact of spatially correlated noise.

It is well known that the GRACE errors are increasing at smaller spatial scales so that the satellite data should not be regarded as a point measure but rather as a spatial average over a region of 100,000 km^2 and larger. Interpolating bilinearly to the position of each sensor as applied during the validation of the simulated OBP is therefore not recommended. Böning et al. (2008) suggested to identify patterns of coherent OBP variability from OGCM simulations and use those regions to average over GRACE data. We therefore calculate autocorrelation maps for each of the in situ stations given in Figure 1 from monthly MPIOM OBP grids covering the

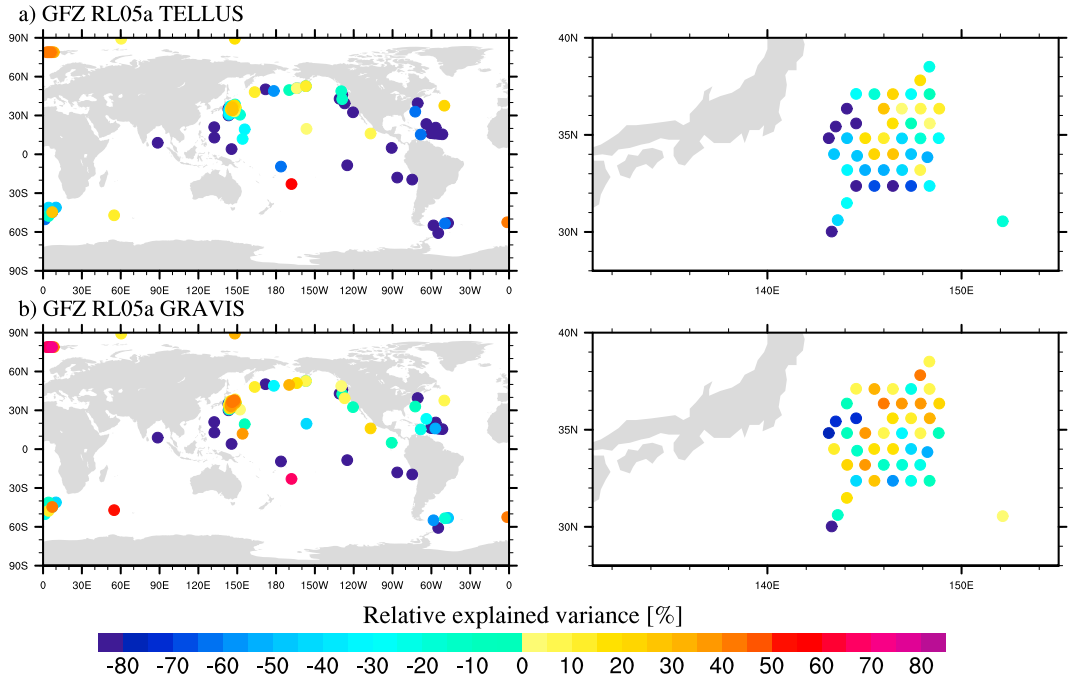

Figure 4. Percentage of variance in ocean bottom pressure observed at in situ stations that is explained by ocean bottom pressure from GRACE monthly Level-3 grids after applying the pattern filter for GFZ Release 05a from TELLUS portal of NASA (a) and for GFZ Release 05a GRAVIS grids (b). GFZ = German Research Centre for Geosciences.

years 2003–2012. All locations with autocorrelation values larger than 0.7 and distances to the in situ station smaller than 2,000 km are included into the area over which GRACE information is averaged to obtain OBP time series that can be compared with the in situ data.

For the relative explained variances of the monthly-mean values (Figure 4) as obtained from the GFZ RL05a GRACE TELLUS solutions, we note relatively poor correspondence between GRACE and in situ OBP, in particular, when compared to the level of fit obtained between in situ data and numerical models as discussed above. Many stations with negative explained variances imply that the residual variance after subtracting GRACE is actually larger than the variance of the in situ observations themselves. Nevertheless, the results are comparable with the results of the validation of the monthly means of the OGCM. For comparison, we also show results of the validation of the new GRAVIS Level-3 grids. Even though both versions of GRACE OBP grids are based on the same Level-2 Stokes coefficients, their correspondence with the in situ data is significantly

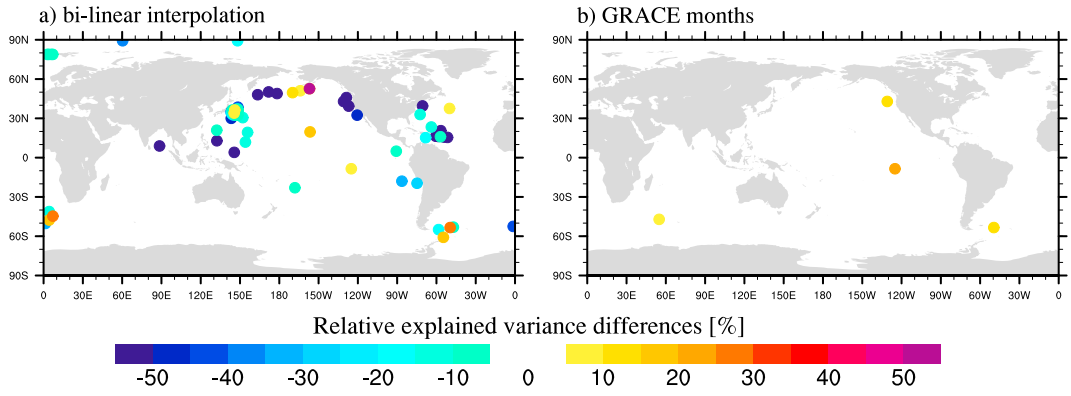

Figure 5. Change in percentage of variance in ocean bottom pressure observed at in situ stations that is explained by ocean bottom pressure derived from GRACE satellite gravimetry compared to Figure 4b after bilinearly interpolating GRACE data to the in situ station's location instead of applying the pattern filter (a), and after considering actual GRACE months instead of the calendar months during the evaluation (b). GRACE = Gravity Recovery and Climate Experiment.

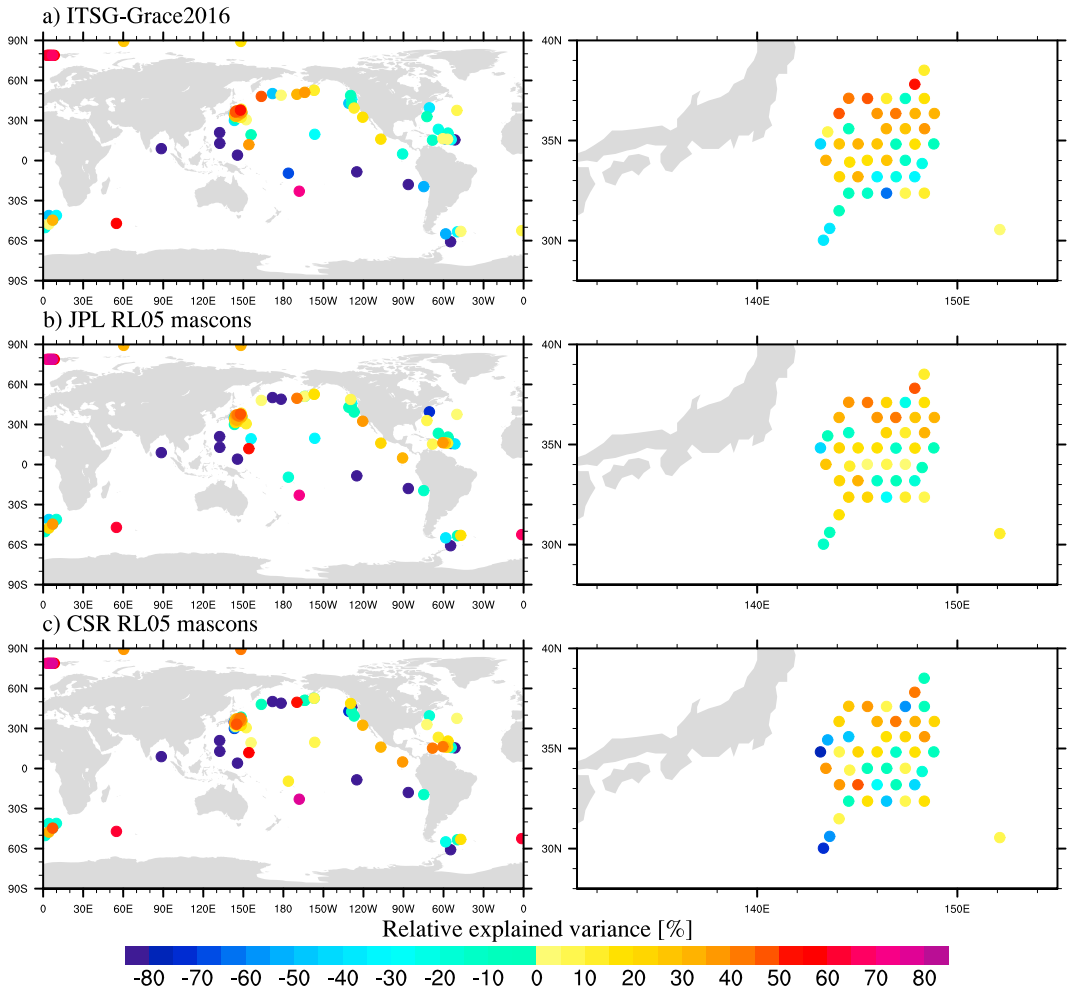

Figure 6. Percentage of variance in ocean bottom pressure observed at in situ stations that is explained by ocean bottom pressure derived from monthly ITSG2016 Stokes coefficients (a); from the JPL RL05 mascon solutions (b); and from the CSR RL05 mascon solutions (c). CSR = Center for Space Research; JPL = Jet Propulsion Laboratory.

different. In the KESS array, almost twice as many data points have positive explained variance for the GRAVIS grid than for TELLUS, which underlines the importance of a careful postprocessing of GRACE solutions prior to any oceanographic interpretation of the satellite record.

When applying bilinear interpolation to the GRACE Level-3 GRAVIS grid instead of the pattern filter (Figure 5a), we note a significant deterioration for many in situ stations. We further note that the full suite of GRACE sensor data is not available every day due to the necessity of satellite swap and orbit-lifting maneuvers; mass trim operations; changes in the temperature control regime; and other interruptions to the science data acquisition that are common to satellites operating in a near-Earth environment. GRACE monthly solutions therefore often do only contain sensor data from a subset of days out of a given month, but only the first and the last day of data used for a particular gravity field are usually provided within the meta data set attached to each gravity field solution. Consequently, we calculate time mean values for the actual *GRACE months* out of the in situ data and recalculate once more relative explained variances (Figure 5b). While in this case improvements compared to using calendar months are visible, those are very modest and present only for some stations with data coverage during those few months (e.g., January 2004) for which the actual GRACE averaging period significantly differs from the calender month. Since, moreover, data gaps in the GRACE sensor data stream are not considered whatsoever—those are expected to have a similar impact—we finally recommend to treat the GRACE monthly means as being referred to the calendar month only.

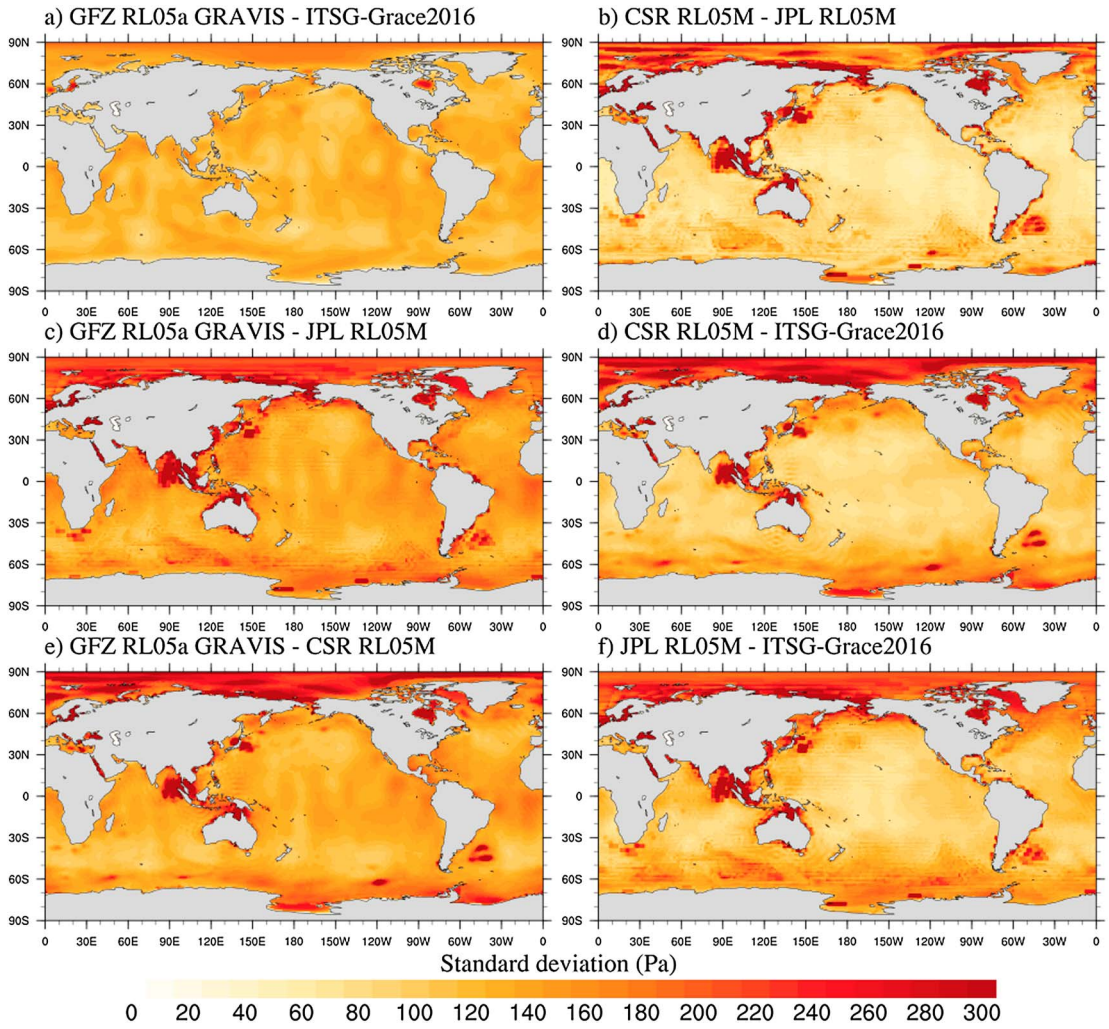

Figure 7. Rms of pair-wise differences of monthly ocean bottom pressure estimates for GFZ RL05a and ITSG-Grace2016 (a); CSR RL05M and JPL RL05M (b); GFZ RL05a and JPL RL05M (c); CSR RL05M and ITSG-Grace2016 (d); GFZ RL05a and CSR RL05M (e); and JPL RL05M and ITSG-Grace2016 (f), each calculated over the period 2003–2012. CSR = Center for Space Research; JPL = Jet Propulsion Laboratory; GFZ = German Research Centre for Geosciences.

5. OBP From Alternative GRACE Solutions

The processing strategy for the GRACE GFZ RL05a solution has been developed around the year 2012 and kept unchanged afterward, so that later months were only added to the time series without making use of more recent insights on sensor data characteristics or parameterization options. A major step forward is only expected from the next reprocessing RL06 that will be made available in late summer 2018. In the meantime, alternative GRACE solutions have been published by various international research groups that make use of numerous improvements in both Level-1 and Level-2 processing methods. Here we assess Stokes coefficients of the ITSG-Grace2016 solutions made available by University of Graz (Mayer-Gürr et al., 2016) processed into OBP by using the same postprocessing strategy as applied to the GFZ RL05a GRAVIS solutions. We further test the RL05 mascon (RL05M) solution of the Center for Space Research (CSR) at the University of Austin (Save et al., 2016), and also the RL05 mascon series as provided by the Jet Propulsion Laboratory (JPL) of NASA (Watkins et al., 2015). For both mascon products, OBP is readily available in gridded format so that no further postprocessing apart from the application of the spatial pattern filter is necessary.

From the validation against in situ OBP (Figure 6), we note slightly better agreement between ITSG2016 and the in situ observations when compared to GFZ RL05a. This is particularly apparent at several stations in the Arctic Ocean and in the Kuroshio Extension region. Both mascon solutions exhibit an even better fit, in particular, in the tropics, where low signal magnitudes due to the strong vertical density changes—and thus

baroclinic compensations of surface-induced pressure gradients—are met by enhanced noise levels in the GRACE solutions caused by the maximum satellite ground track separation distance at the equator.

It is instructive to also calculate over the period 2003–2012 pair-wise monthly differences of all four considered GRACE products and compare the resulting rms fields (Figure 7). For the two Stokes coefficient solutions GFZ RL05a and ITSG-Grace2016, we note a globally rather homogeneous spread of about 1.5 hPa that differs only slightly from region to region. Notable exceptions are some semienclosed regions as Hudson Bay, Baltic, and North Sea, where deficits of the GRACE nontidal atmosphere and ocean dealiasing product AOD1B RL05 are (partially) compensated in ITSG-Grace2016 by coestimated daily fields from a Kalman Smoother approach as described in Kurtenbach et al. (2012). We further note that differences in the open ocean are smallest between the two mascon series with a remaining noise floor of less than 1 hPa in the Central Pacific. Errors in ITSG-Grace2016 in that area are only slightly larger, whereas GFZ RL05a shows scatter of about 1.5 hPa.

It is, however, interesting to note that for selected regions very different results are obtained from the mascon solutions when compared to the Stokes coefficients products. This includes regions of major offshore earthquakes as the Sumatra-Andaman event from the year 2004, or the Tohoku-Oki rupture in 2011. Both mascon parameterization obviously respond very differently to the coseismic change in the gravity field. Also, dynamics of the Argentine Gyre are known to be not reproduced by the AOD1B and thus mapped into the monthly GRACE gravity fields. CSR RL05 M approximately captures the time variable rotation structure of the gyre as known from high-resolution ocean models and satellite altimetry, whereas the JPL mascon solutions reveal a spatially rather heterogeneous response. Also, individual pixels in the Amundsen and Ross Sea show enhanced variability in the JPL series that cannot be explained by GRACE sensor data characteristics. Close to the coasts, the somewhat different treatment of spatial leakage from the continents causes further discrepancies among the different releases. A notable exception is Arafura Sea northward of Australia, where differences extend much further offshore to be only related to typical leakage problems.

Figure 7 thus indicates many regions where individual GRACE gravity field estimation choices taken by the different processing centers lead to substantial discrepancies in the resulting OBP estimates, and where it is advisable to assess more than one GRACE solutions from preferably different processing centers for particular oceanographic applications. The figure could be also used as a guideline for selecting future in situ observation stations that would be most helpful for GRACE validation activities. Unfortunately, many regions with above average GRACE uncertainties are also characterized by harsh environmental conditions that are rather challenging for the collection of in situ data even today.

6. Conclusions

In situ OBP provides a very precise measure of ocean mass redistribution due to a variety of different dynamical processes acting on very different temporal and spatial scales. Data from 154 different locations scattered over all ocean basins has been contrasted for five different frequency bands against a recent experiment from a global ocean general circulation model. We found almost no agreement between model and observations at periods below 24 hr due to underestimation of variability in the model, sensor noise, and remaining tidal signals in the in situ station data. Consistency between model and observations is rapidly increasing for longer periods, culminating in positive explained variances at every single station considered for periods between 3 and 10 days. The correspondence is decreasing again toward longer periods, where dynamic processes typically not considered in an OGCM as the barystatic sea level variability become increasingly important and the in situ time series are affected by systematic effects in the instruments associated to aging of the oscillator and consequently drift in the measurements; local subsidence of the instrument on the seafloor; and the need for surface maintenance and subsequent redeployment at regular time intervals.

When looking at monthly-mean estimates only, the correspondence of in situ bottom pressure with results from the GRACE satellite mission is, however, worse than the fit with the numerical model, even though large-scale barystatic mass changes are known to be monitored by the GRACE mission quite accurately. We conclude that it is particularly related to the residual spatially correlated errors in the GRACE record. A revised postprocessing strategy as applied for the gridded GRACE data disseminated via the newly launched GRAVIS portal of GFZ improves the fit in many areas. Similarly, the consideration of the exact start and end days of each monthly solution improves the fit at a few stations. It is, however, suspected that data gaps in the GRACE sensor data stream within the month have a quite similar effect, but this information is not readily

available from the current Level-2 GRACE products and has to be obtained from the corresponding processing center directly. The fit between in situ observations and GRACE is further improved with more recent data releases as ITSG-Grace2016 and the mascon solutions from both JPL and CSR. However, the analysis of pairwise differences revealed substantial discrepancies between individual solutions at places with particular ocean dynamics as in the Argentine Gyre or underneath the Antarctic ice shelves, thereby reflecting the individual gravity field estimation strategies of the different processing centers.

In view of the strong high-frequency component of the GRACE-based OBP, it is argued that a higher temporal resolution of the oceanic GRACE product would be rather advantageous. Efforts in providing such higher temporal sampling have been reported from both European (Kurtenbach et al., 2009, 2012) and U.S. research groups (Save et al., 2016). To only identify the barystatic contribution to sea level changes, a monthly sampling of the GRACE fields appears to be sufficient, but for the determination of the wind-driven ocean circulation contributions to the bottom pressure field, the effects of inadequate temporal filtering limit the applicability of the present-day gravity fields.

Acknowledgments
We thank Jennifer Bonin, the second anonymous reviewer, and the Editor Don P. Chambers for their very helpful feedback on our manuscript. In situ OBP data collected by AWI Bremerhaven is available from the PANGEA database. MPIOM model data is accessible from isdc.gfz-potsdam.de/esmdata. All numerical simulations were performed at Deutsches Klimarechenzentrum in Hamburg, Germany. GRACE TELLUS ocean data were processed by Don P. Chambers, supported by the NASA MEaSUREs Program, and are available at http://grace.jpl.nasa.gov. GRACE GRAVIS data are publicly available from gravis.gfz-potsdam.de. This work has been supported by Deutsche Forschungsgemeinschaft under grant D01311/3-1.

References

A, G., Wahr, J., & Zhong, S. (2013). Computations of the viscoelastic response of a 3-D compressible Earth to surface loading: An application to glacial isostatic adjustment in Antarctica and Canada. *Geophysical Journal International*, *192*(2), 557–572. https://doi.org/10.1093/gji/ggs030

Bergmann-Wolf, I., Zhang, L., & Dobslaw, H. (2014). Global eustatic sea-level variations for the approximation of geocenter motion from GRACE. *Journal of Geodetic Science*, *4*(1), 37–48. https://doi.org/10.2478/jogs-2014-0006

Bingham, R. J., & Hughes, C. W. (2008a). The relationship between sea-level and bottom pressure variability in an eddy permitting ocean model. *Geophysical Research Letters*, *35*, L03602. https://doi.org/10.1029/2007GL032662

Bingham, R. J., & Hughes, C. W. (2008b). Determining North Atlantic meridional transport variability from pressure on the western boundary: A model investigation. *Journal of Geophysical Research*, *113*, C09008. https://doi.org/10.1029/2007JC004679

Bishop, S. P., & Watts, D. R. (2014). Rapid eddy-induced modification of subtropical mode water during the Kuroshio Extension System study. *Journal of Physical Oceanography*, *44*(7), 1941–1953. https://doi.org/10.1175/JPO-D-13-0191.1

Böning, C., Timmermann, R., Macrander, A., & Schröter, J. (2008). A pattern-filtering method for the determination of ocean bottom pressure anomalies from GRACE solutions. *Geophysical Research Letters*, *35*, L18611. https://doi.org/10.1029/2008GL034974

Boyer, T., Levitus, S., Garcia, H., Locarnini, R. A., Stephens, C., & Antonov, J. (2005). Objective analyses of annual, seasonal, and monthly temperature and salinity for the World Ocean on a 0.25° grid. *International Journal of Climatology*, *25*(7), 931–945. https://doi.org/10.1002/joc.1173

Chambers, D. P. (2006). Evaluation of new GRACE time-variable gravity data over the ocean. *Geophysical Research Letters*, *33*, L17603. https://doi.org/10.1029/2006GL027296

Chambers, D. P. (2012). GRACE monthly ocean mass grids NETCDF Release 5.0. Ver. 5.0, PO.DAAC, dataset accessed [2017-05-30] at https://doi.org/10.5067/TEOCN-0N005

Cheng, M., & Ries, J. (2013). Monthly estimates of C20 from 5 SLR satellites based on GRACE RL05 models, Grace Technical Note 07 (Tech. Rep.). Austin, TX: Center for Space Research.

Cheng, M., Ries, J. C., & Tapley, B. D. (2011). Variations of the Earth's figure axis from satellite laser ranging and GRACE. *Journal of Geophysical Research*, *116*, B01409. https://doi.org/10.1029/2010JB000850

Dahle, C., Gruber, C., Fagiolini, E., & Flechtner, F. (2016). Gravity field mapping from GRACE: Different approaches—Same results? In N. Sneeuw, et al. (Eds.), *VIII HOTINE-MARUSSI SYMPOSIUM ON MATHEMATICAL GEODESY* (Vol. 142, pp. 165–175). Cham, Switzerland: Springer. International Association of Geodesy Symposia. https://doi.org/10.1007/1345_2015_8

Dobslaw, H., Bergmann-Wolf, I., Dill, R., Poropat, L., & Thomas, M. (2017). A new high-resolution model of non-tidal atmosphere and ocean mass variability for de-aliasing of satellite gravity observations: AOD1B RL06. *Geophysical Journal International*, *211*, 263–269. https://doi.org/10.1093/gji/ggx302

Flechtner, F., Neumayer, K.-H., Dahle, C., Dobslaw, H., Fagiolini, E., Raimondo, J.-C., & Güntner, A. (2016). What can be expected from the GRACE-FO laser ranging interferometer for earth science applications? *Surveys in Geophysics*, *37*(2), 457–470. https://doi.org/10.1007/s10712-015-9338-y

Howe, B. M., & Workshop Participants (2015). From space to the deep seafloor: Using SMART submarine cable systems in the ocean observing system, Report of NASA Workshops, 9–10 October 2014, Pasadena, CA, and 26–28 May 2015, Honolulu, HI, SOEST Contribution 9549.

Jungclaus, J. H., Fischer, N., Haak, H., Lohmann, K., Marotzke, J., Matei, D., et al. (2013). Characteristics of the ocean simulations in the Max Planck Institute Ocean Model (MPIOM) the ocean component of the MPI-Earth system model. *Journal of Advances in Modeling Earth Systems*, *5*, 422–446. https://doi.org/10.1002/jame.20023

Kurtenbach, E., Eicker, A., Mayer-Gürr, T., Holschneider, M., Hayn, M., Fuhrmann, M., & Kusche, J. (2012). Improved daily GRACE gravity field solutions using a Kalman smoother. *Journal of Geodynamics*, *59-60*, 39–48. https://doi.org/10.1016/j.jog.2012.02.006

Kurtenbach, E., Mayer-Gürr, T., & Eicker, A. (2009). Deriving daily snapshots of the Earth's gravity field from GRACE L1B data using Kalman filtering. *Geophysical Research Letters*, *36*, L17102. https://doi.org/10.1029/2009GL039564

Kusche, J., Schmidt, R., Petrovic, S., & Rietbroek, R. (2009). Decorrelated GRACE time-variable gravity solutions by GFZ, and their validation using a hydrological model. *Journal of Geodesy*, *83*(10), 903–913. https://doi.org/10.1007/s00190-009-0308-3

Macrander, A., Böning, C., Boebel, O., & Schröter, J. (2010). Validation of GRACE gravity fields by in-situ data of ocean bottom pressure, *System Earth via geodetic-geophysical space techniques*. Berlin: Springer.

Mayer-Gürr, T., Behzadpour, S., Ellmer, M., Kvas, A., Klinger, B., & Zehentner, N. (2016). ITSG-Grace2016—Monthly and daily gravity field solutions from GRACE, GFZ Data Services. https://doi.org/10.5880/icgem.2016.007

McCarthy, G. D., Smeed, D. A., Johns, W. E., Frajka-Williams, E., Moat, B. I., Rayner, D., et al. (2015). Measuring the Atlantic meridional overturning circulation at 26°N. *Progress in Oceanography*, *130*, 91–111. https://doi.org/10.1016/j.pocean.2014.10.006

Meinig, C., Stalin, S., Nakamura, A., & Milburn, H. (2005). Real-time deep-ocean tsunami measuring, monitoring, and reporting system: The NOAA DART II description and disclosure.

Meredith, M. P., Woodworth, P. L., Chereskin, T. K., Marshall, D. P., Allison, L. C., Bigg, G. R., et al. (2011). Sustained monitoring of the Southern Ocean at Drake Passage: Past achievements and future priorities. *Reviews of Geophysics*, *49*, RG4005. https://doi.org/10.1029/2010RG000348

Milburn, H., Nakamura, A., & Gonzalez, F. (1996). Real-time tsunami reporting from the deep ocean. In *Proceedings of the Oceans 96 MTS/IEEE Conference 23-26* (pp. 390–394). Fort Lauderdale, FL. September 1996.

Nowlin, W. D., Whitworth, T. III., & Pillsbury, R. D. (1977). Structure and transport of the Antarctic circumpolar current at Drake Passage from short-term measurements. *Journal of Physical Oceanography*, *7*, 788–802. https://doi.org/10.1175/1520-0485(1977)007<0788:SATOTA>2.0.CO;2

Paulson, A., Zhong, S., & Wahr, J. (2007). Inference of mantle viscosity from GRACE and relative sea level data. *Geophysical Journal International*, *171*(2), 497–508. https://doi.org/10.1111/j.1365-246X.2007.03556.x

Pawlowicz, R., Beardsley, B., & Lentz, S. (2002). Classical tidal harmonic analysis including error estimates in MATLAB using T_TIDE. *Computers & Geosciences*, *28*, 929–937. https://doi.org/10.1016/S0098-3004(02)00013-4

Ray, R. D. (2013). Precise comparisons of bottom-pressure and altimetric ocean tides. *Journal of Geophysical Research: Oceans*, *118*, 4570–4584. https://doi.org/10.1002/jgrc.20336

Ray, R. D., & Erofeeva, S. Y. (2014). Long-period tidal variations in the length of day. *Journal of Geophysical Research: Solid Earth*, *119*, 1498–1509. https://doi.org/10.1002/2013JB010830

Save, H., Bettadpur, S., & Tapley, B. D. (2016). High-resolution CSR GRACE RL05 mascons. *Journal of Geophysical Research: Solid Earth*, *121*, 7547–7569. https://doi.org/10.1002/2016JB013007

Swenson, S., Chambers, D. P., & Wahr, J. (2008). Estimating geocenter variations from a combination of GRACE and ocean model output. *Journal of Geophysical Research*, *113*, B08410. https://doi.org/10.1029/2007JB005338

Swenson, S., & Wahr, J. (2006). Post-processing removal of correlated errors in GRACE data. *Geophysical Research Letters*, *33*, L08402. https://doi.org/10.1029/2005GL025285

Tamisiea, M. E., Hill, E. M., Ponte, R. M., Davis, J. L., Velicogna, I., & Vinogradova, N. T. (2010). Impact of self-attraction and loading on the annual cycle in sea level. *Journal of Geophysical Research*, *115*, C07004. https://doi.org/10.1029/2009JC005687

Tanaka, Y., Suzuki, T., Imanishi, Y., Okubo, S., Zhang, X., Ando, M., et al. (2018). Temporal gravity anomalies observed in the Tokai area and a possible relationship with slow slips. *Earth, Planets and Space*, *70*, 25. https://doi.org/10.1186/s40623-018-0797-5

Tapley, B. D., Bettadpur, S., Watkins, M., & Reigber, C. (2004). The gravity recovery and climate experiment: Mission overview and early results. *Geophysical Research Letters*, *31*, L09607. https://doi.org/10.1029/2004GL019920

Watkins, M., Wiese, D., Yuan, D.-N., Boening, C., & Landerer, F. (2015). Improved methods for observing Earth's time variable mass distribution with GRACE using spherical cap mascons. *Journal of Geophysical Research: Solid Earth*, *120*, 2648–2671. https://doi.org/10.1002/2014JB011547

Watts, D., & Kontoyiannis, H. (1990). Deep-ocean bottom pressure measurement—Drift removal and performance. *Journal of Atmospheric and Oceanic Technology*, *7*(2), 296–306. https://doi.org/10.1175/1520-0426(1990)007<0296:DOBPMD>2.0.CO;2